Supporting Information

Continuous nucleation of metallic nanoparticles via photocatalytic reduction

Zoe C. Simon,[a] Ann Marie N. Paterno,[a] Kaitlyn M. McHugh,[a] Paige J. Moncure,[a] Riti Sen,[a] Samuel T. Patton,[a] Eric M. Lopato,[b] Savannah Talledo,[b] Stefan Bernhard,[b] Jill E. Millstone[a, c, d]*

a. Department of Chemistry, University of Pittsburgh, Pittsburgh, Pennsylvania 15260, United States.
b. Department of Chemistry, Carnegie Mellon University, Pittsburgh, Pennsylvania 15213, United States.
c. Department of Chemical and Petroleum Engineering, University of Pittsburgh, Pittsburgh, Pennsylvania 15260, United States.
d. Department of Chemical and Petroleum Engineering, University of Pittsburgh, Pittsburgh, Pennsylvania 15260, United States.
e. Department of Mechanical Engineering and Materials Science, University of Pittsburgh, Pittsburgh, Pennsylvania 15260, United States.

Table of Contents:

Experimental Section

Materials. Hydrogen tetrachloroaurate(III) trihydrate ($HAuCl_4 \cdot 3H_2O$, 99.999%), copper(II) bromide ($CuBr_2$, 99%), silver nitrate ($AgNO_3$, 99.9999%), palladium(II) chloride ($PdCl_2$, 99.9%), cadmium nitrate tetrahydrate ($Cd(NO_3)_2 \cdot 4H_2O$, 98%), iron(III) chloride hexahydrate ($FeCl_3 \cdot 6H_2O$, 97%), cobalt(II) nitrate hexahydrate ($Co(NO_3)_2 \cdot 6H_2O$, ≥98%), nickel(II) chloride hexahydrate ($NiCl_2 \cdot 6H_2O$, 99.9999%), chloroplatinic acid solution (H_2PtCl_6, 8 wt. % in H_2O), triethanolamine (TEOA, 98%), 2-(4-fluorophenyl)-5-methylpyridine (≥95%), 4,4′-di-tert-butyl-2,2′-dipyridyl (98%), and iridium(III) chloride ($IrCl_3$, 99.8%) were purchased from Sigma-Aldrich (St. Louis, MO). Poly(ethylene glycol) methyl ether thiol (PEGSH, average MW = 1 kDa) was purchased from Laysan Bio, Inc. (Arab, AL). All reagents were used as received unless otherwise indicated. NANOpure (Thermo Scientific, ≥18.2 MΩ·cm) water was used to prepare all aqueous solutions.

Synthesis of NPs via photocatalytic reduction. Our unique parallel photoreactor design used to synthesize all photocatalytic reduction NPs has been described previously.[1, 2] Briefly, all reaction samples are housed in 1 mL glass shell vials and illuminated from below by two 100 W blue light-emitting diodes (LEDs, Chanzon High Power Led Chip 100 W, 440−450 nm/3000 mA/DC 30−34 V). Reactions were run at a total volume of 408 µL consisting of 90 µL total metal salt solutions (all at a concentration of 4.17 mM), 144 µL acetonitrile, 34 µL of PEGSH (at a concentration of 11 mM), 100 µL of a 0.275 mM solution of the photosensitizer (PS), $[Ir(Fmppy)_2dtbbpy]PF_6$ (where Fmppy → 4'-fluoro-2-phenyl-5-methylpyridine, and dtbbpy → 4,4'-di-tert-butyl-2,2'-bipyridine, synthesized according to literature[3]), and, lastly, 40 µL of a 60% (w/w) solution of triethanolamine (TEOA) in acetonitrile, added in that order. All solutions were made with acetonitrile as the solvent. Solution vials were capped and promptly placed in the photoreactor for illumination. Though the vials were capped for the duration of the reaction, the reactions proceeded in an air atmosphere.

Transmission Electron Microscopy (TEM). NP solutions were prepared for TEM by washing 5 times using 10 kDa molecular weight cutoff filters (Amicon Ultra centrifugal filter units, EMD Millipore) at 4000 rcf for 10 min (Eppendorf centrifuge 5804R with swing bucket rotor A-4−44). An aliquot of the washed samples was then drop cast onto a carbon-backed 200 mesh Cu or Ni TEM grid (Ted Pella, Inc.) and dried under ambient conditions. A Hitachi H-9500 microscope operating at 300 kV (Nanoscale Fabrication and Characterization Facility, Petersen Institute of Nanoscience and Engineering, University of Pittsburgh, PA) was used for all imaging. Images were analyzed using Digital Micrograph v2.10.1282.0 (Gatan, Inc.) and/or ImageJ v 1.47d (National Institutes of Health, USA) software.

Ultraviolet-visible-Near-Infrared (UV-vis-NIR) Extinction Spectroscopy. NPs were characterized by UV-vis-NIR extinction spectroscopy using a Cary 5000 spectrophotometer (Agilent, Inc.). Spectra were baseline corrected to the spectrum of

H_2O. Spectra were collected by adding 200 µL of unwashed NP solution to 800 µL of water. Quartz cuvettes (Hellma, Inc.) with a 1 cm path length were used in all analyses.

Inductively Coupled Plasma Optical Emission Spectrometry (ICP-OES). ICP-OES analysis was performed using an argon flow with an Agilent 5100 VDV ICP-OES (Department of Civil and Environmental Engineering, University of Pittsburgh). An aqua regia solution (3:1 ratio of hydrochloric acid to nitric acid) was prepared using ultrapure reagents (Sigma-Aldrich, HCl > 99.999% trace metal basis; HNO_3 > 99.999% trace metal basis), a portion of which was then diluted with NANOpure water to yield a 5% v/v aqua regia matrix. A 5% v/v nitric acid matrix was used for all sample analysis containing silver. After washing the NPs 5 times using 10 kDa molecular weight cutoff filters, an aliquot (~200 µL) was dissolved overnight in ~100 µL of the concentrated aqua regia or nitric acid solution and then diluted to 3 mL with the 5% aqua regia or 5% nitric acid solution and analyzed via ICP-OES to determine metal concentration. Unknown metal concentrations were determined by comparison to a 7-point standard curve with a range of 0.10–10 ppm of each metal (0.10, 0.50, 1.0, 2.5, 5.0, 7.5, and 10 ppm) prepared by volume using ICP standards (Fluka, TraceCERT 1000 ± 2 mg/L metal in HNO_3), all diluted in a 5% aqua regia or nitric acid matrix. The Ag standards were prepared separately to avoid the formation of AgCl. All standards and unknown samples were measured 3 times and averaged. A 3 min flush time with 5% nitric acid matrix was used between all runs, and a blank was analyzed before each unknown sample to confirm removal of all residual metals from the instrument.

Caution: aqua regia is highly toxic and corrosive and should only be used with proper personal protective equipment and training. Aqua regia should be handled inside a fume hood only.

No irradiation control experiments. If NP formation only occurs during irradiation, then a change in optical density (O.D.) of the solution should only be observed during irradiation. To investigate this claim we analyzed the extinction spectrum of reaction mixtures which were not irradiated, but instead were kept in the dark for 10 minutes, 1, 4, and 24 h and then analyzed (Figure S1). In these spectra, it is clear that only at 24 hours in the dark, do we begin to detect even traces of nanoparticle formation, likely from the reaction of the Au precursor and the thiolated ligand which are known to react together to form small quantities of particles over long timescales.

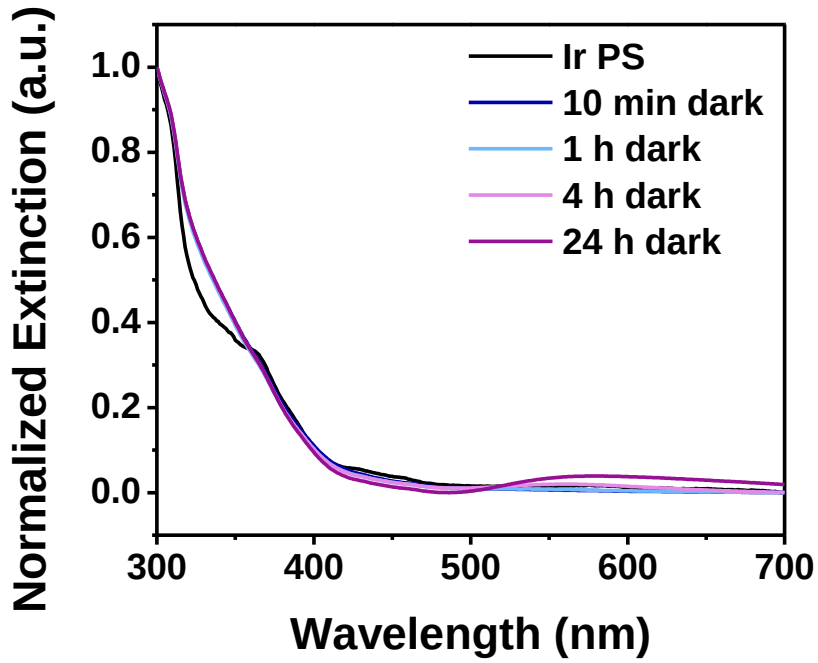

Figure S1. Extinction spectra of the photosensitizer and samples that were not irradiated and kept in the dark for 10 min, 1 h, 4 h, and 24 h showing NP formation does not occur in the dark. In these spectra, it is clear that no particle formation or growth is detected when the solution is not irradiated until 24 hours in the dark, at which point we begin to detect small traces of chemical reaction, likely from the reaction of the Au precursor and the thiolated ligand, which are known to react together to form small quantities of particles over long timescales (N.B. no particles were isolable from any of the timepoints). Absorption in the spectra beginning around 400 nm is due to the photosensitizer.

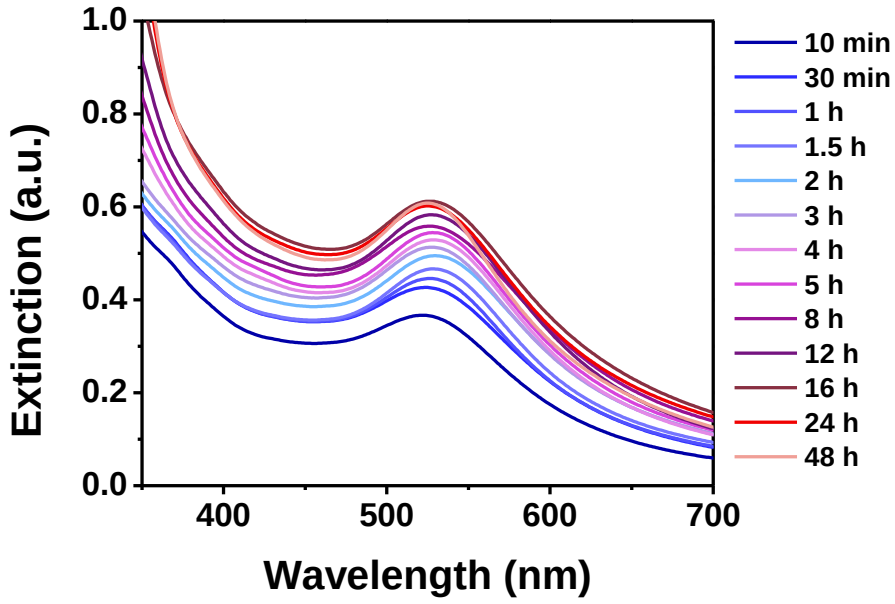

Figure S2. Extinction spectra of Au NPs synthesized by photocatalytic reduction from 10 min to 48 h of irradiation.

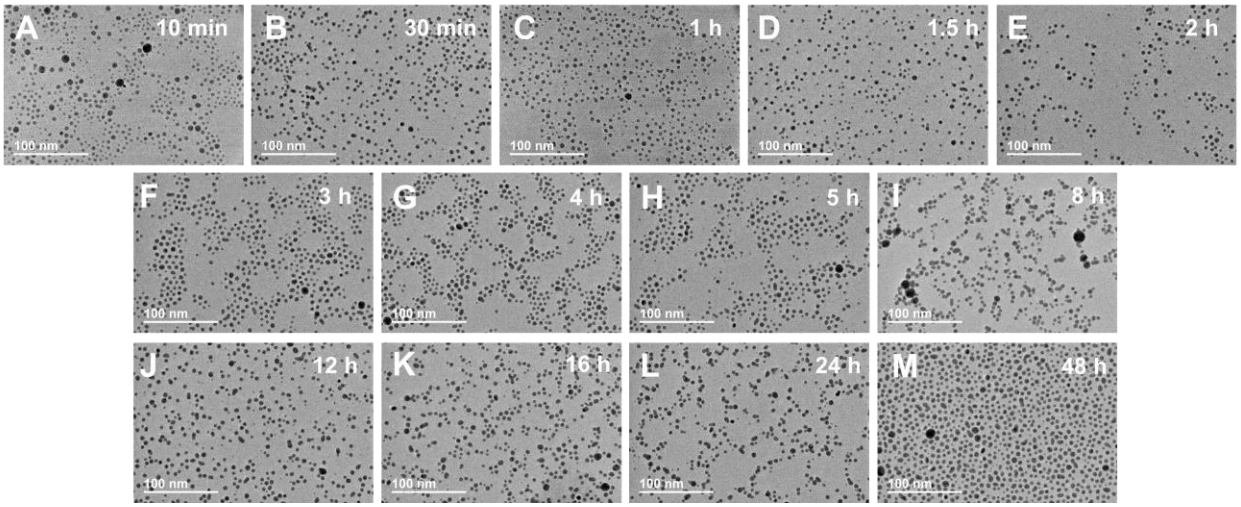

Figure S3. Representative TEM micrographs of Au NPs synthesized by photocatalytic reduction from 10 min to 48 h of irradiation.

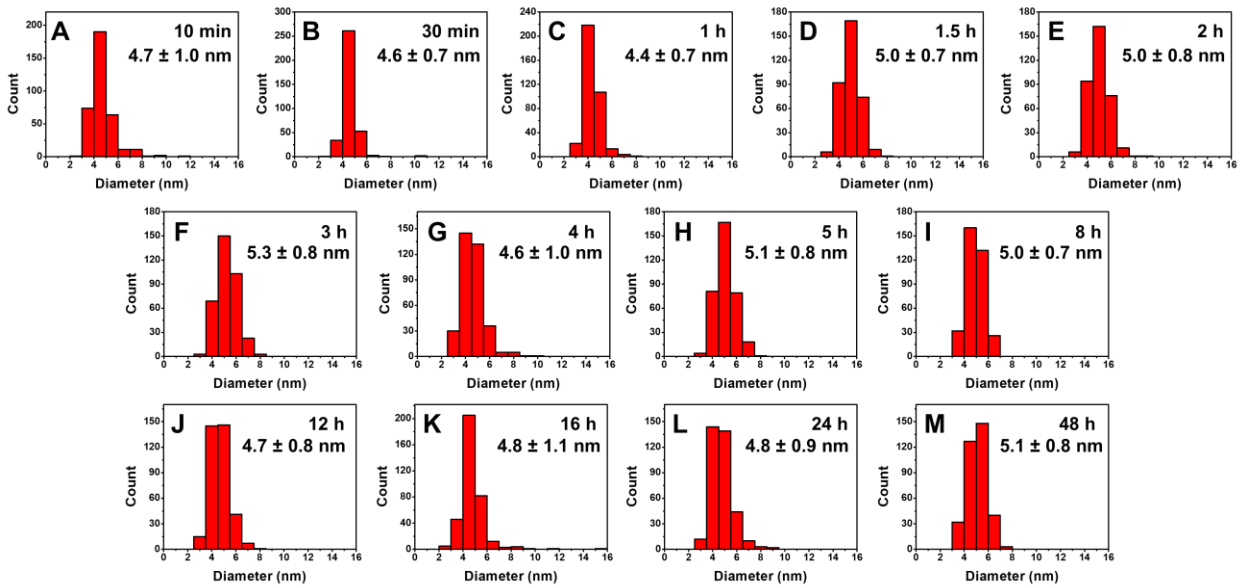

Figure S4. Size histograms and average NP diameters of Au NPs synthesized by photocatalytic reduction from 10 min to 48 h of irradiation (N ≥ 350).

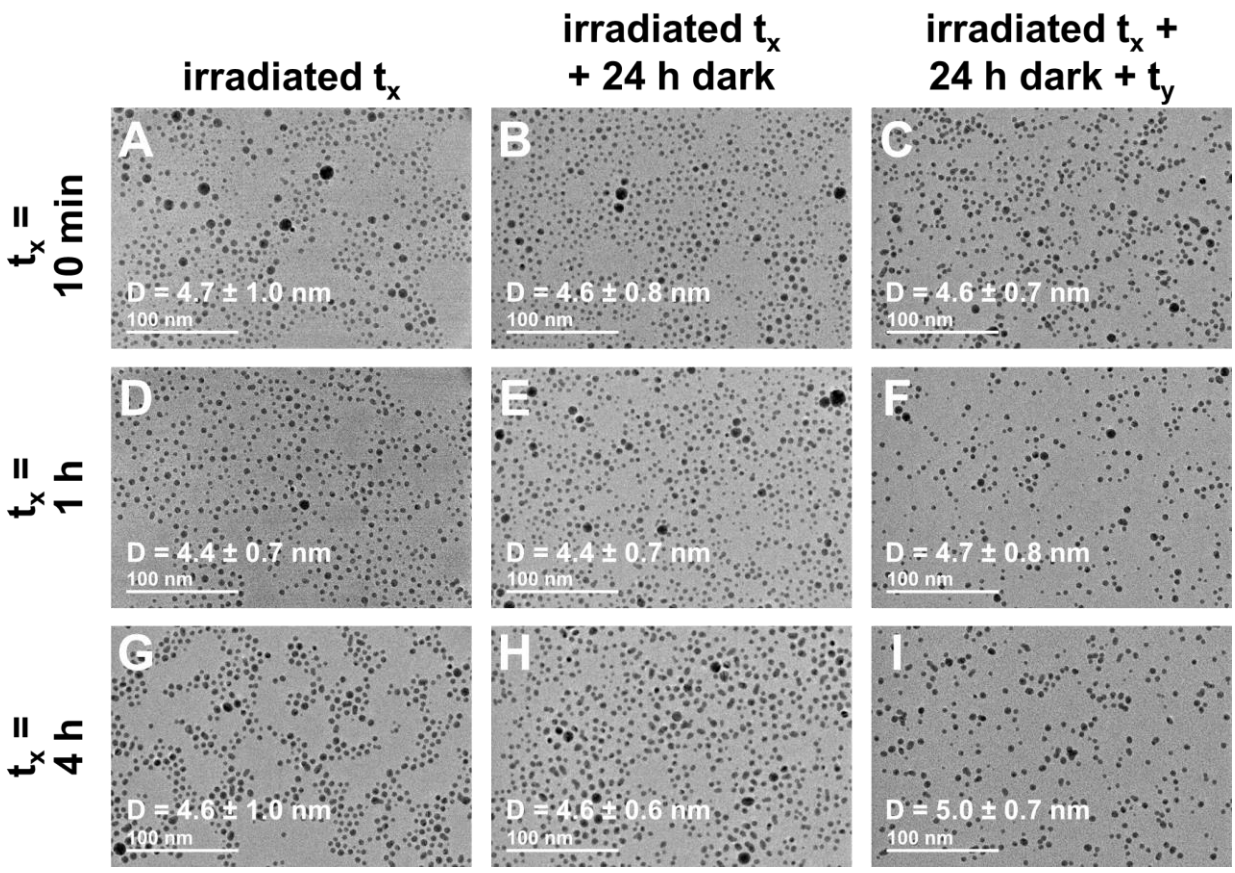

Figure S5. Representative TEM micrographs of Au NPs synthesized by photocatalytic reduction after (A, D, G) continuous irradiation for t_x (t_x = 10 min, 1 h, 4 h), (B, E, H) irradiation for t_x followed by 24 h in the dark, and (C, F, I) irradiation for t_x, followed by 24 h in the dark, and then reintroduced to irradiation for t_y, such that $t_x + t_y$ = 24 h of total irradiation time.

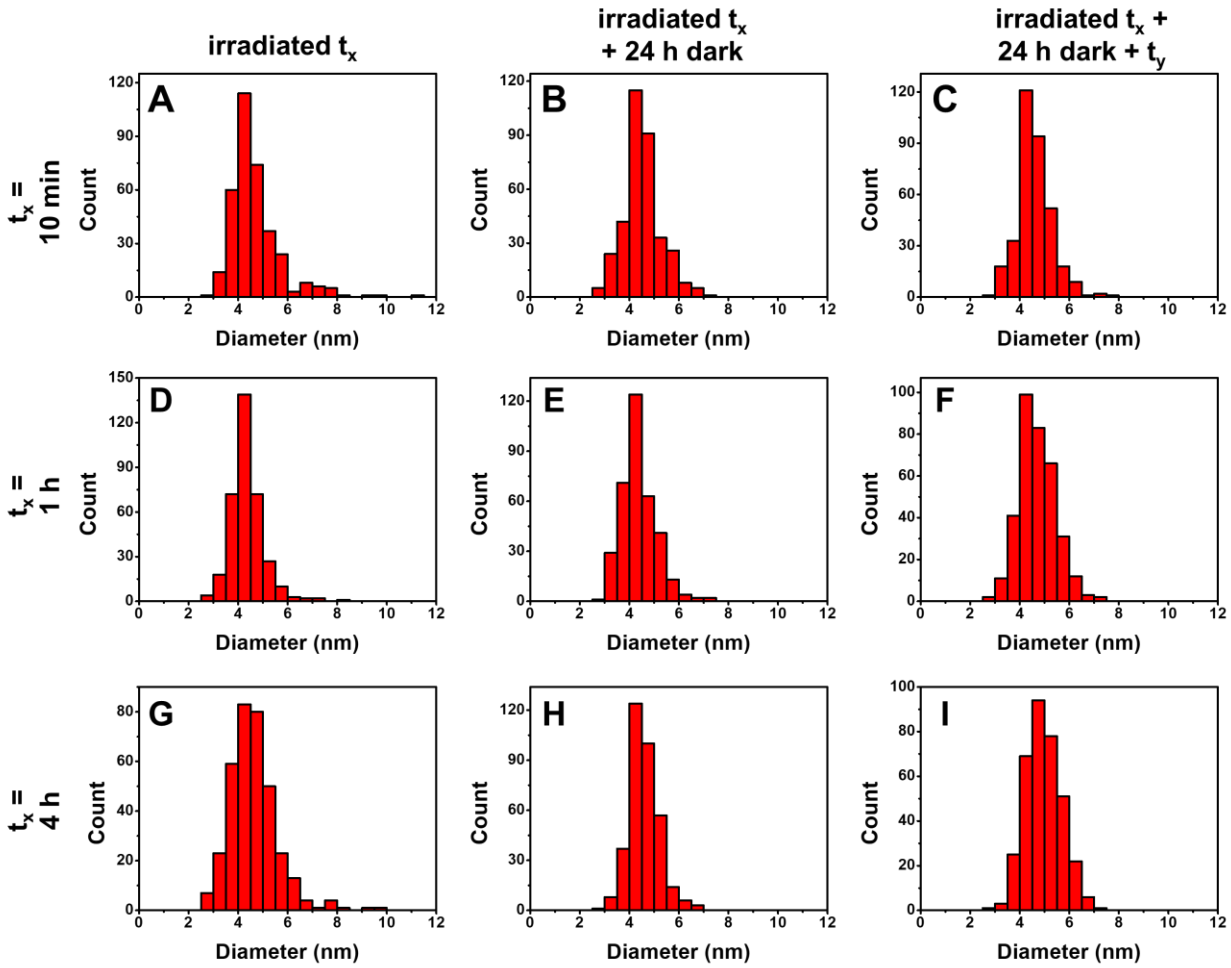

Figure S6. Size histograms of Au NPs synthesized by photocatalytic reduction after (A, D, G) continuous irradiation for t_x (t_x = 10 min, 1 h, 4 h), (B, E, H) irradiation for t_x followed by 24 h in the dark, and (C, F, I) irradiation for t_x, followed by 24 h in the dark, and then reintroduced to irradiation for t_y, such that $t_x + t_y$ = 24 h of total irradiation time.

Change in optical density as a function of irradiation interval. In Figure 2B, we show the O.D. of the NP solutions at λ_{max} as a function of irradiation time, where this O.D. can be used as a relative representation of particle yield in the reaction. The error bars in the figure represent the standard error of at least three independent trials, and these data demonstrate that there is good consistency in particle yield for any given duration of continuous illumination. However, under conditions of discontinuous irradiation, such as the experiments shown in Figure 3, there is slight variation between the particle yield and the particle yield under continuous illumination of the same duration (Figure S7; gray bars compared to light blue, light purple, and light red bars). However, all particle yields from discontinuous illumination are similar to one another. Taken together, these results are consistent with the controls shown in Figure S1, which indicate that by 24 h in the dark there is likely some reaction between the Au precursor and the thiolated ligand. This reaction results in a slightly lower NP yield at 24 h of total

irradiation in discontinuous irradiation experiments compared to 24 h of continuous irradiation.

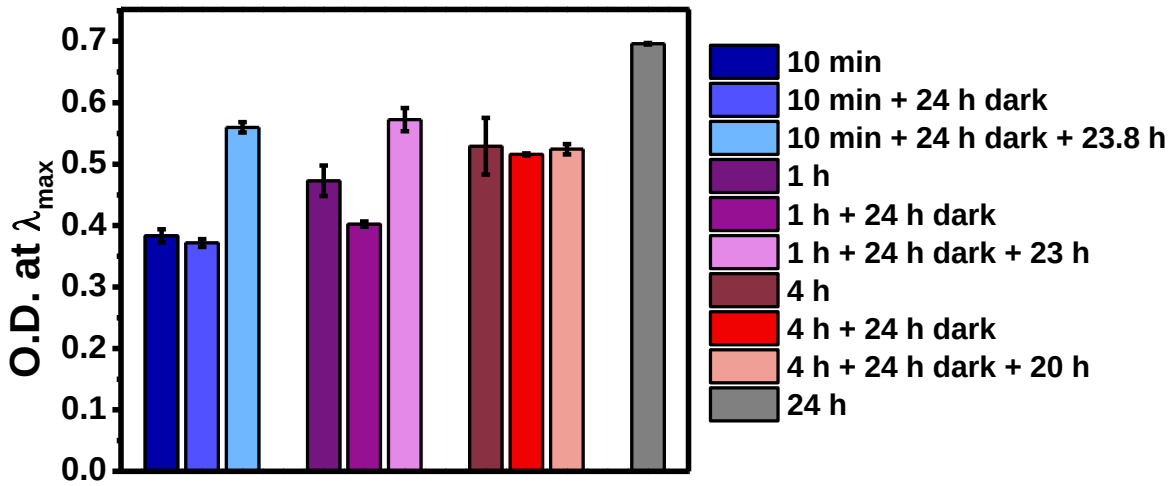

Figure S7. Optical density of Au NPs at λ_{max} as a function of irradiation interval. Navy, dark purple, maroon, and gray bars represent the O.D. when the solution is continuously irradiated for 10 min, 1 h, 4 h, and 24 h, respectively. Mid-tone blue, purple, and red bars represent samples analyzed after irradiation followed by 24 h in the dark. Light blue, purple, and red bars represent the O.D. after the solutions are reintroduced to irradiation after 24 h in the dark, for a total irradiation time of 24 h. Error bars represent the standard error of at least three independent trials.

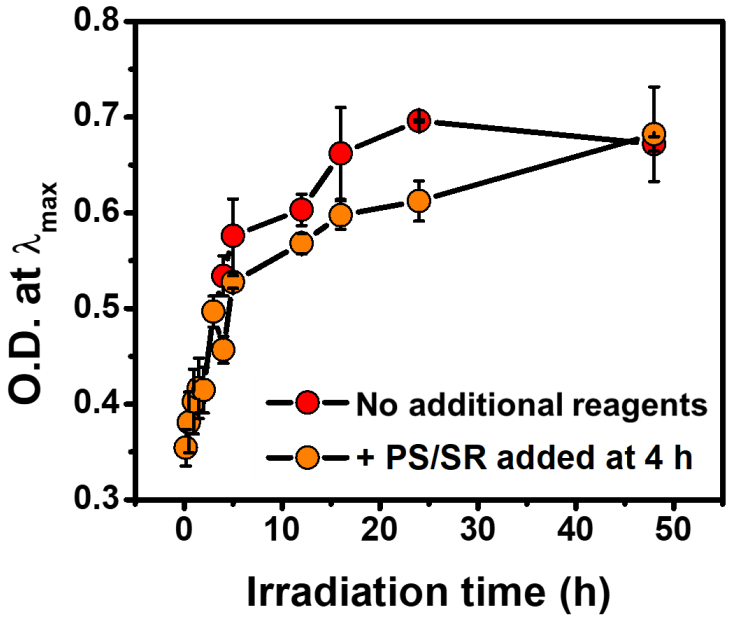

Figure S8. Optical density of Au NPs at λ_{max} as a function of irradiation time when no additional reagents are added to the reaction vial (red) and when the PS and SR are replenished at 4 h (orange, 100 µL of PS and 40 µL SR). The addition of both PS and SR do not result in an increase in NP formation rate.

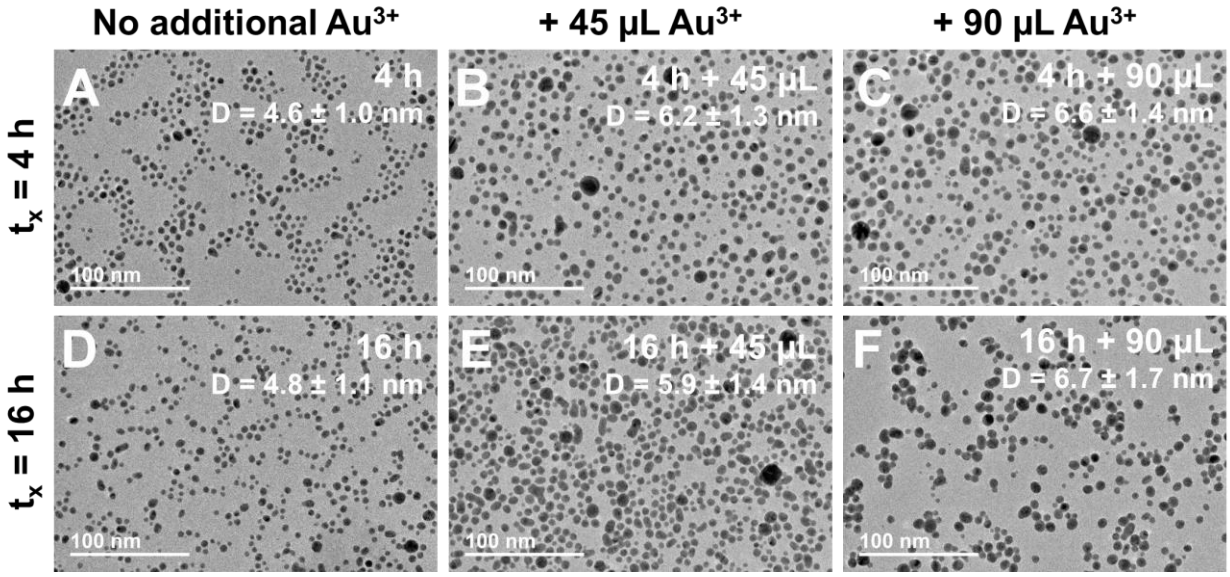

Figure S9. Representative TEM micrographs and average NP diameters of Au NPs synthesized by photocatalytic reduction after (A, D) no additional Au^{3+} was added, the addition of (B, E) 45 µL of Au^{3+} and (C, F) 90 µL of Au^{3+} after (B, C) 4 h and (E, F) 16 h of irradiation.

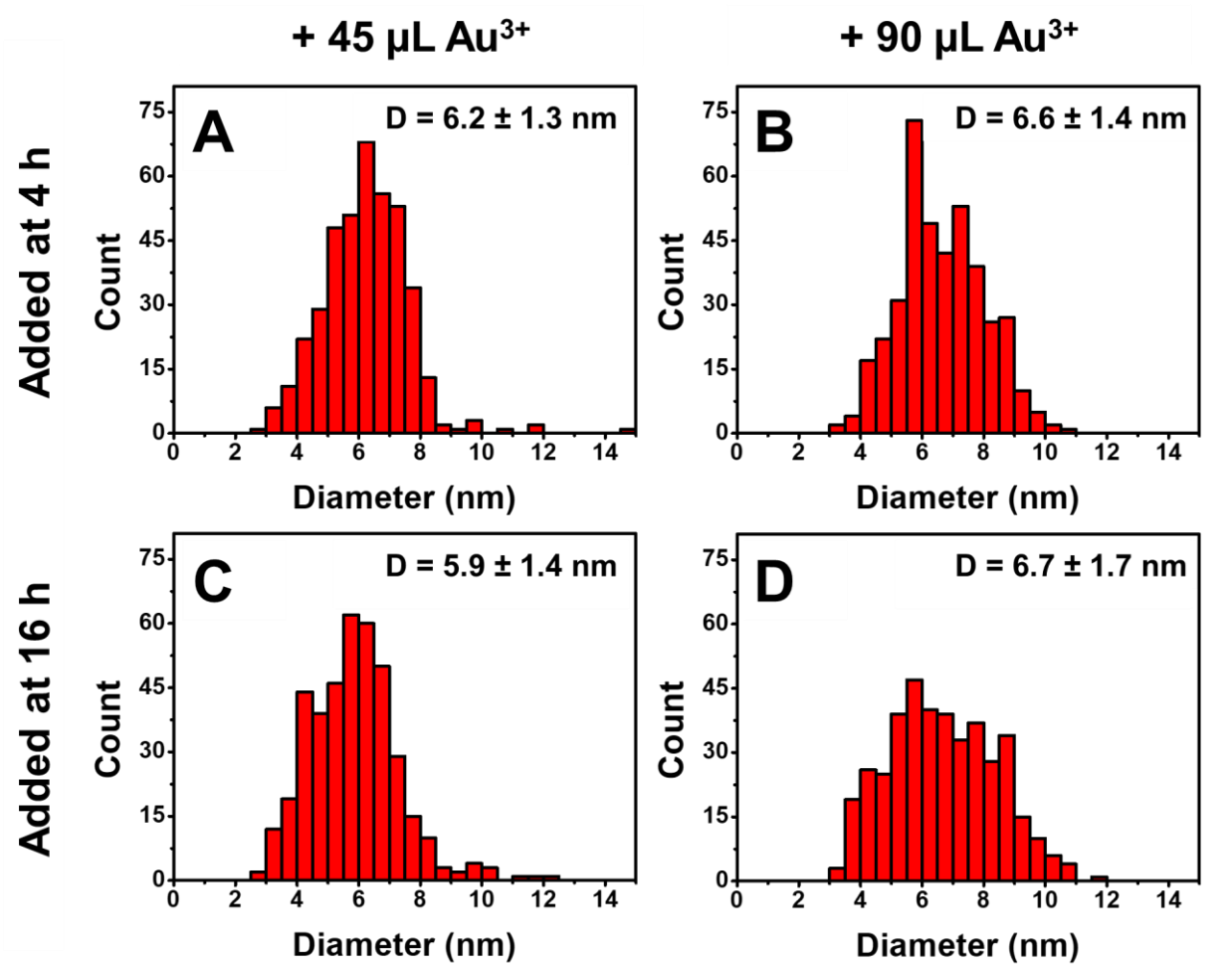

Figure S10. Size histograms and NP diameters of Au NPs synthesized by photocatalytic reduction with (A, C) 45 or (B, D) 90 µL of additional Au^{3+} added at (A, B) 4 h or (C, D) 16 h of irradiation (N ≥ 350).

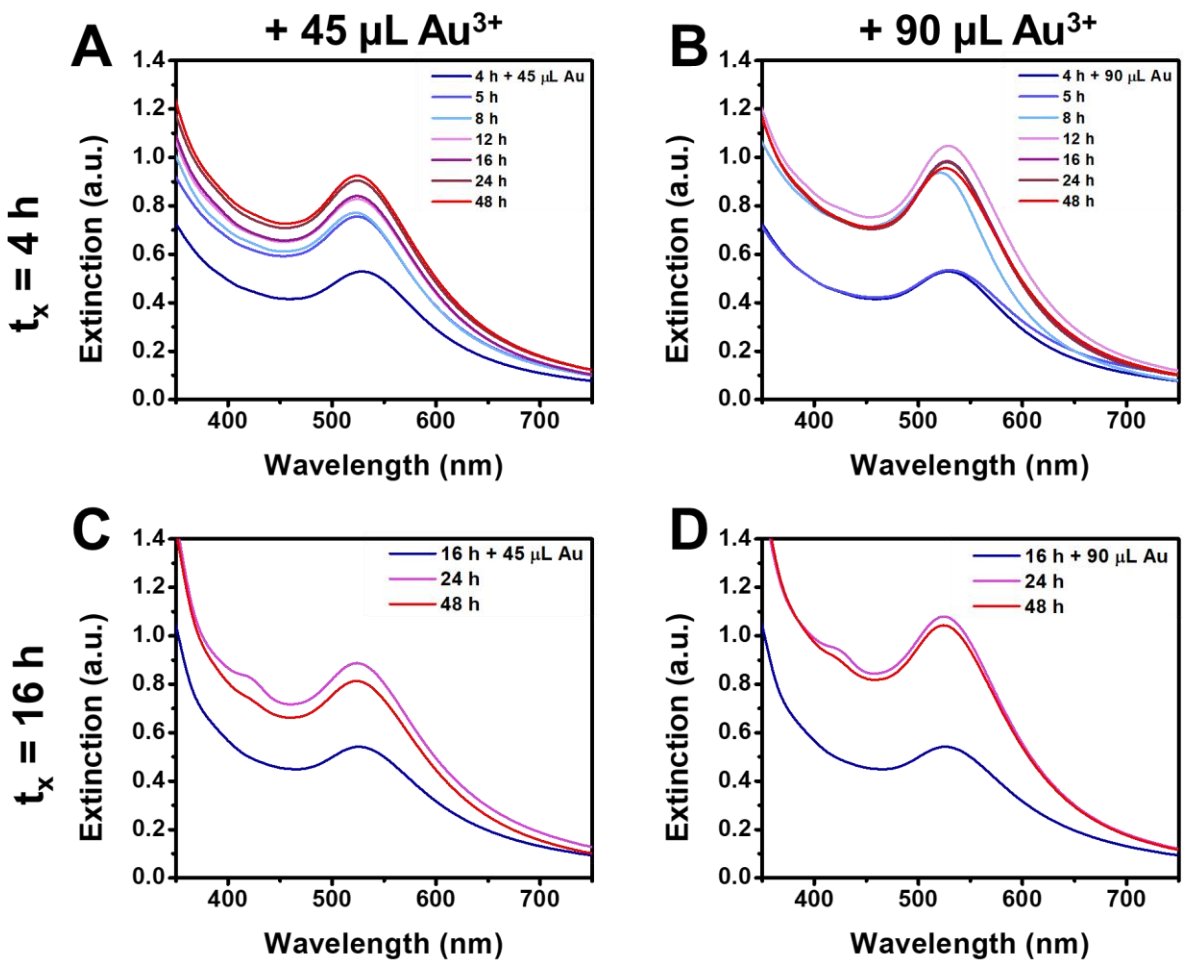

Figure S11. Extinction spectra of Au NPs synthesized by photocatalytic reduction after the addition of (A, C) 45 µL of Au^{3+} and (B, D) 90 µL of Au^{3+} after (A, B) 4 h and (C, D) 16 h of irradiation.

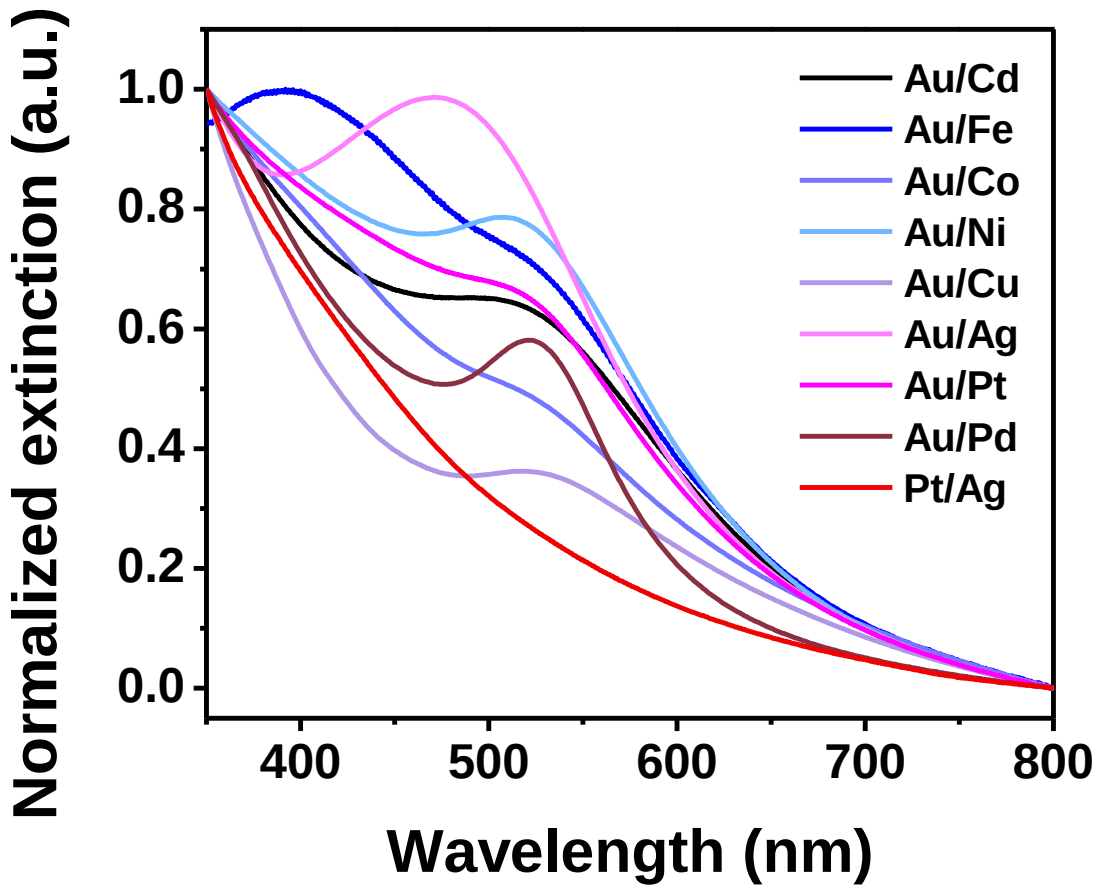

Figure S12. Extinction spectra of bimetallic NPs synthesized by photocatalytic reduction with a 1:1 initial stoichiometric molar ratio after 1 h of irradiation.

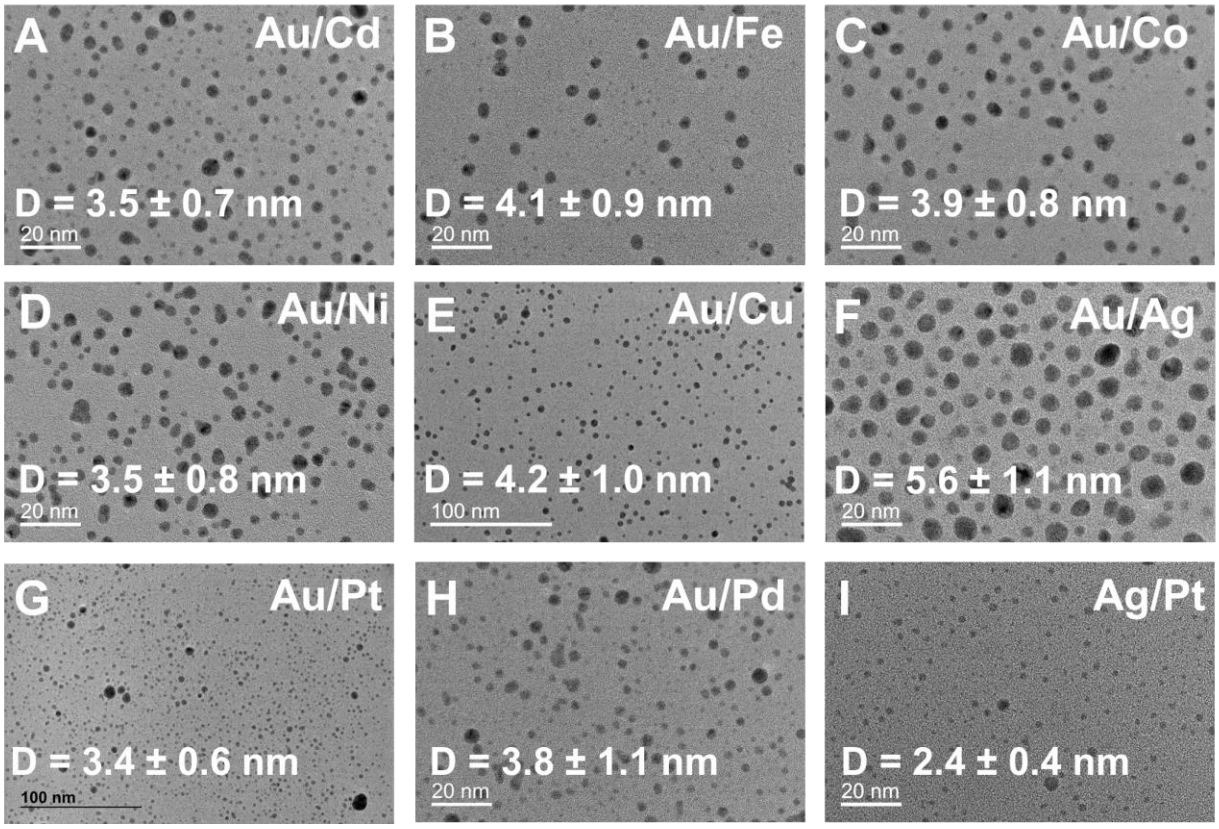

Figure S13. Representative TEM micrographs of bimetallic NPs synthesized by photocatalytic reduction with a 1:1 initial stoichiometric molar ratio after 1 h of irradiation.

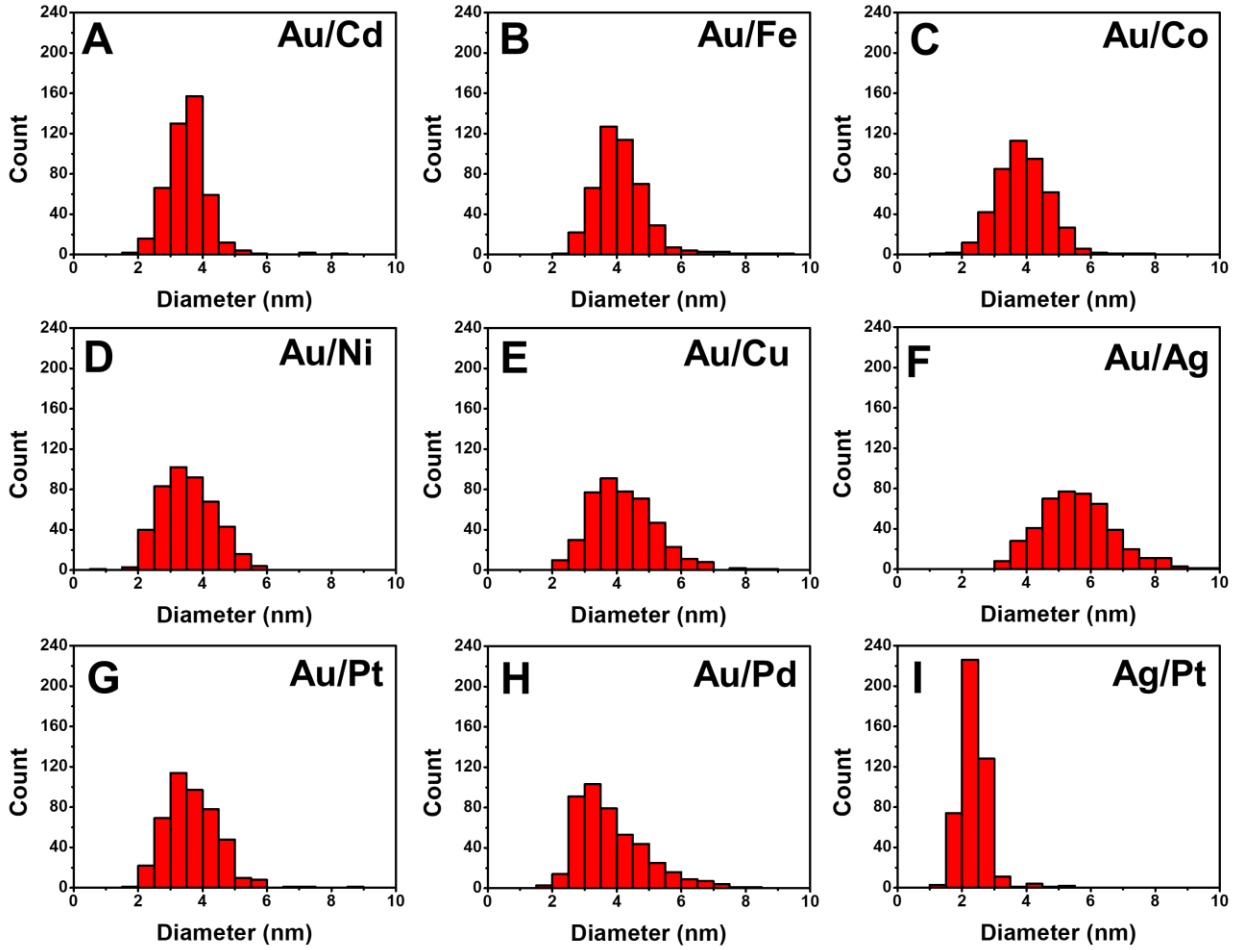

Figure S14. Size histograms of bimetallic NPs synthesized by photocatalytic reduction with a 1:1 initial stoichiometric molar ratio after 1 h of irradiation (N ≥ 450).

Table S1. Metal incorporation of bimetallic NPs synthesized by photocatalytic reduction with a 1:1 initial stoichiometric molar ratio after 1 h of irradiation. Averages are measured from three independent trials ± the standard error.

Sample	% Secondary Metal Incorporated
Au/Cd	1.5 ± 0.1
Au/Fe	0 ± 0
Au/Co	5.0 ± 0.8
Au/Ni	6.3 ± 0.3
Au/Cu	15.0 ± 1.8
Au/Ag	31.9 ± 2.7
Au/Pt	12.7 ± 2.6
Au/Pd	36.2 ± 1.7
Ag/Pt	55.3 ± 3.6

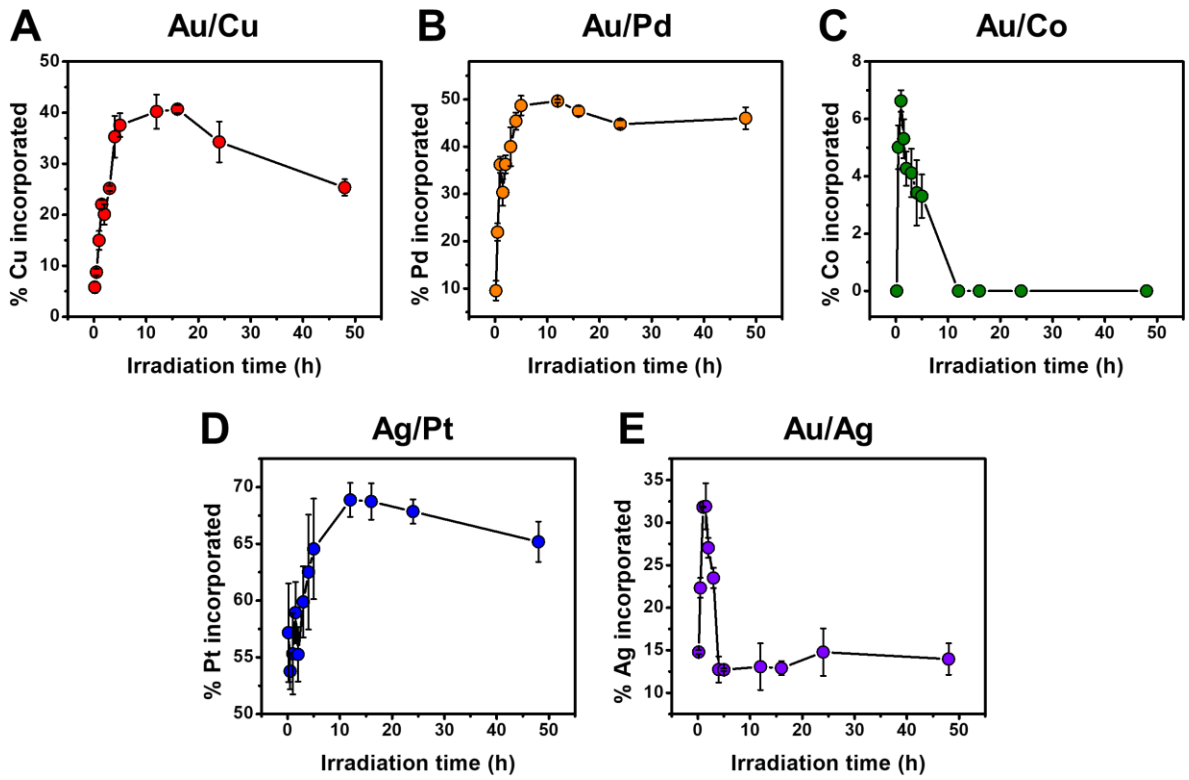

Figure S15. Metal incorporation measured by ICP-OES for (A) Au/Cu, (B) Au/Pd, (C) Au/Co, (D) Ag/Pt, and (E) Au/Ag from 10 min to 48 h of irradiation. Error bars represent the standard error of at least three independent trials. We hypothesize that the difference in incorporation trajectories for the different metal combinations is driven by the stability and photosensitivity of NPs enriched in the secondary metal. For example, Au/Ag exhibits a steep decrease in Ag content, suggesting Ag rich NPs are prone to degradation in solution. The metal incorporation as a function of irradiation time data is omitted for Au/Ni, Au/Fe, and Au/Cd because secondary metal incorporation by 1 h of irradiation is approximately 0%. This result is also true for the Au/Co system, which we show as representative of these 4 systems. The incorporation trajectory for Au/Co demonstrates that over the course of the reaction the metal incorporation remains low (peaking at 6.6% Co), indicating that for these 4 systems it is unlikely that the secondary metal will incorporate within the 48 h experiment.

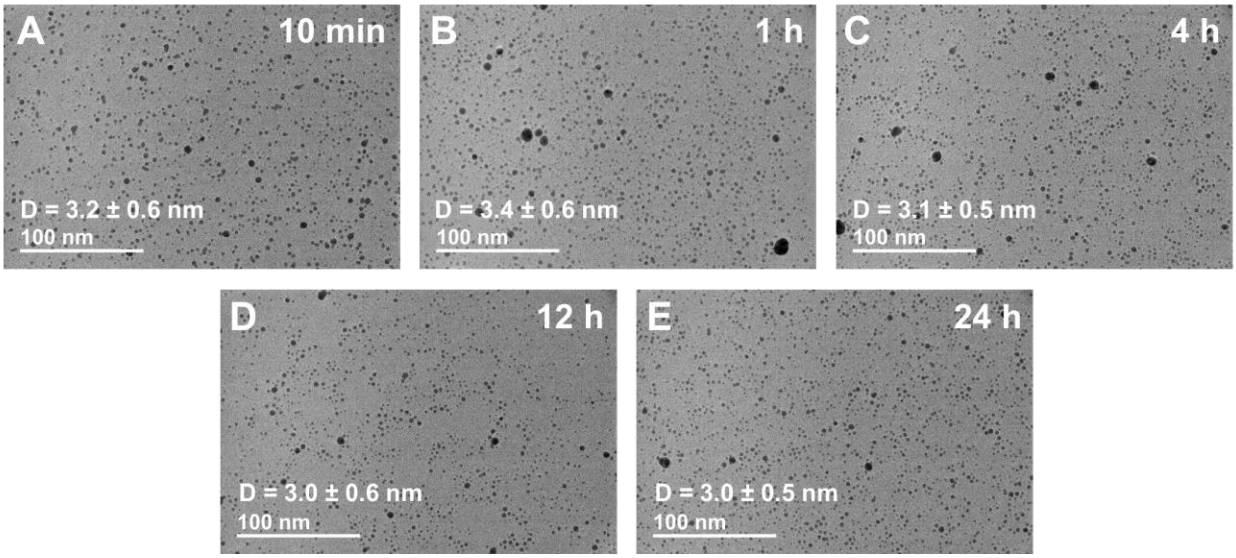

Figure S16. Representative TEM micrographs of Au/Pt NPs synthesized by photocatalytic reduction with a 1:1 initial stoichiometric molar ratio after irradiation for (A) 10 min, (B) 1 h, (C) 4 h, (D) 12 h, and (E) 24 h.

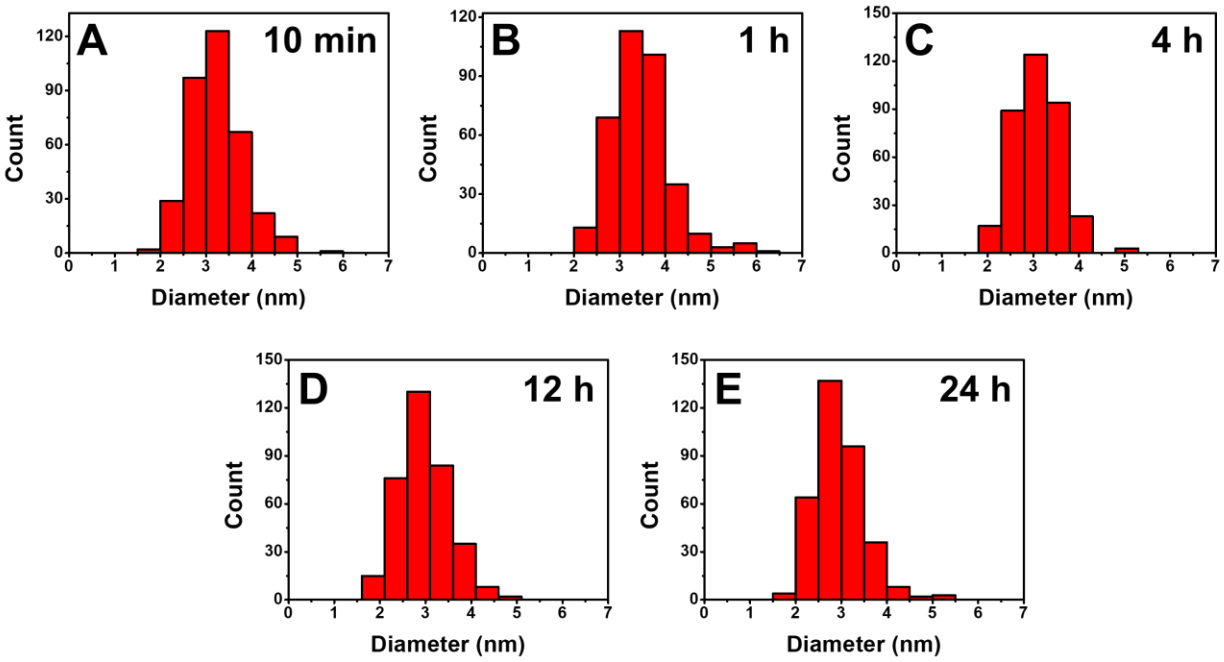

Figure S17. Size histograms of Au/Pt NPs synthesized by photocatalytic reduction with a 1:1 initial stoichiometric molar ratio after irradiation for (A) 10 min, (B) 1 h, (C) 4 h, (D) 12 h, and (E) 24 h (N ≥ 350).

Uniformity of plate illumination control. Previous studies using this photoreactor have shown the distribution in light intensity to be uniform across the plate using hydrogen evolution experiments including both reaction yield and reaction kinetics.[1, 4, 5] We include here additional control experiments specifically relevant to our study. In order to test the uniformity of light across the plate and eliminate the possibility of the effect an uneven distribution of illumination may have on our experiments, we conducted and compared the same light-driven reaction at different positions on the plate and measured reaction yield. Below we show that the illumination intensity across the vials is uniform by conducting a control experiment measuring the optical density of the same reaction solutions at 1 h of irradiation at 13 positions across the plate (Figures S18-S19).

Positions of the test vials were chosen based on the placement of the vials used in this study. For each time experiment shown in our report, we analyzed 13 time points of irradiation. A control vial was placed at each of these 13 positions, containing the same reaction solution used to produce Au nanoparticles. All vials were irradiated for 1 h, then analyzed by extinction spectroscopy. We demonstrate good fidelity in O.D. measured at each position, and calculated an average O.D. and standard error of 0.342 ± 0.004. Not only is there little variation measured in the average O.D. (on the order of the error in the instrument detection itself), but also there is no consistent skew of O.D. across the plate (Figure S19B), indicating that there is not unequal illumination on one side of the plate versus the other.

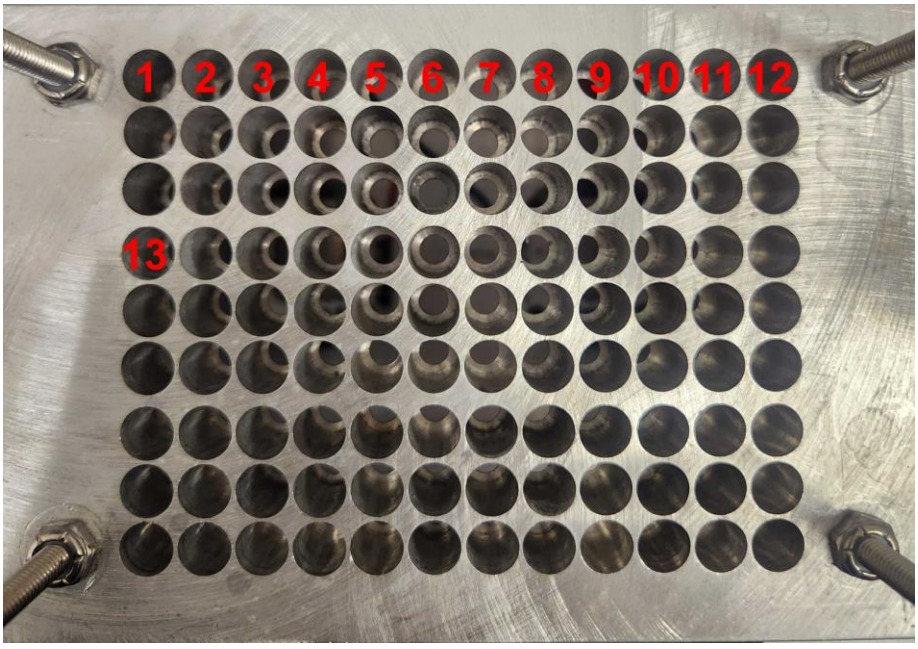

Figure S18. Image of the photoreactor plate with the 13 vial positions tested in the uniformity of illumination experiment numbered in red. These positions were chosen because all reactions in this report are run in these wells on the plate.

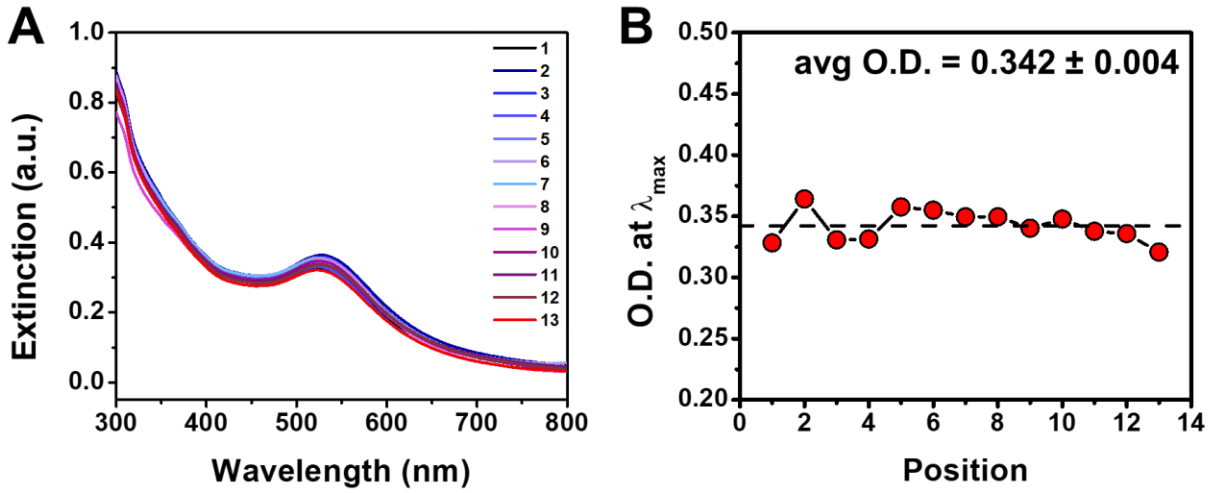

Figure S19. (A) Extinction spectra of Au NPs after 1 h of irradiation at 13 positions across the photoreactor. (B) Corresponding O.D. at λ_{max} showing no consistent skew of O.D. values across the reactor plate.

References

1. Lopato, E. M.; Eikey, E. A.; Simon, Z. C.; Back, S.; Tran, K.; Lewis, J.; Kowalewski, J. F.; Yazdi, S.; Kitchin, J. R.; Ulissi, Z. W.; Millstone, J. E.; Bernhard, S., Parallelized screening of characterized and DFT-modeled bimetallic colloidal cocatalysts for photocatalytic hydrogen evolution. *ACS Catal.* **2020,** *10* (7), 4244-4252.
2. Simon, Z. C.; Lopato, E. M.; Bhat, M.; Moncure, P. J.; Bernhard, S. M.; Kitchin, J. R.; Bernhard, S.; Millstone, J. E., Ligand enhanced activity of in situ formed nanoparticles for photocatalytic hydrogen evolution. *ChemCatChem* **2022,** *14* (2), e202101551.
3. Curtin, P. N.; Tinker, L. L.; Burgess, C. M.; Cline, E. D.; Bernhard, S., Structure−activity correlations among iridium (III) photosensitizers in a robust water-reducing system. *Inorg. Chem.* **2009,** *48* (22), 10498-10506.
4. Motz, R. N.; Lopato, E. M.; Connell, T. U.; Bernhard, S., High-throughput screening of Earth-abundant water reduction catalysts toward photocatalytic hydrogen evolution. *Inorg. Chem.* **2021,** *60* (2), 774-781.
5. Mdluli, V.; Diluzio, S.; Lewis, J.; Kowalewski, J. F.; Connell, T. U.; Yaron, D.; Kowalewski, T.; Bernhard, S., High-throughput synthesis and screening of iridium (III) photocatalysts for the fast and chemoselective dehalogenation of aryl bromides. *ACS Catal.* **2020,** *10* (13), 6977-6987.